# Nanostructured Titania−Polymer Photovoltaic Devices Made Using PFPE-Based Nanomolding Techniques

Stuart S. Williams,[♦,†] Meredith J. Hampton,[♦,†] Vignesh Gowrishankar,[‡] I-Kang Ding,[‡] Joseph L. Templeton,[†] Edward T. Samulski,[†] Joseph M. DeSimone,*[,†] and Michael D. McGehee*[,‡]

*Department of Chemistry, Campus Box 3290, University of North Carolina at Chapel Hill, Chapel Hill, North Carolina 27599 and Department of Materials Science and Engineering, Stanford University, 476 Lomita Mall, Stanford, California 94305-4045*

*Received March 12, 2008. Revised Manuscript Received May 27, 2008*

We fabricated ordered bulk heterojunction photovoltaic (PV) cells using a perfluoropolyether (PFPE) elastomeric mold to control the donor−acceptor interfacial morphology within devices. Anatase titania nanostructures with postlike features ranging from 30 to 100 nm in height and 30 to 65 nm in spacing were fabricated using the Pattern Replication In Nonwetting Templates (PRINT) process. The nanostructured devices showed a 2-fold improvement in both short-circuit current ($J_{sc}$) and power conversion efficiency (PCE) relative to reference bilayer cells. Additionally, the titania was functionalized with Z907 dye to increase both the short-circuit current ($J_{sc}$) and open-circuit voltage ($V_{oc}$). As a result we observed a device efficiency ($\eta_{eff}$) of 0.6%, the highest recorded efficiency value so far for an imprinted titania−P3HT device.

## Introduction

Conjugated polymers are promising photovoltaic materials because they are strong light absorbers and solution processable and can be deposited onto flexible substrates at low cost. To date, the most efficient polymeric solar cell utilizes a disordered bulk heterojunction (Figure 1a) in which the conjugated polymer is mixed with an electron acceptor.[1–3] During processing, the mixture automatically phase separates into nanoscale domains with a length scale on the order of the exciton diffusion length, maximizing the exciton collection efficiency. Unfortunately, when we use different material systems, the phase separation distance might change. The morphology of the blend depends critically on numerous processing variables, such as the side chain length of the polymer, weight ratio of materials, choice of solvents, molecular weight, regioregularity, and annealing conditions.[4,5] Even when we have a phase separation length scale on the order of the exciton diffusion length, each phase in the blends may contain dead ends, which could hamper the charge collection efficiency.

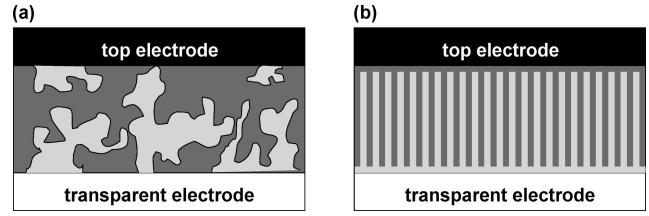


**Figure 1.** Device architectures of conjugated polymer-based photovoltaic cells: (a) disordered bulk heterojunction and (b) ordered bulk heterojunction. Adopted from ref 11.

Ordered bulk heterojunctions (Figure 1b) made by filling inorganic nanostructures with organic semiconductors have distinct advantages over their disordered counterparts because the morphology can be precisely controlled.[6–10] Metal oxide ($TiO_2$, ZnO, etc.) templates can be fabricated with continuous pathways or pores on the scale of the exciton diffusion length in the organic semiconductor. Consequently, the device possesses the ideal morphology for maximizing charge collection efficiency regardless of the polymer used.

Titania is an attractive material for ordered bulk heterojunction photovoltaic cells for many reasons: it is abundant and nontoxic, it has a low-lying conduction band that can

* To whom correspondence should be addressed. J.M.D.: phone, (919) 962-2166; e-mail, desimone@unc.edu. M.D.M.: phone, (650) 736-0307; e-mail. mmcgehee@stanford.edu.
♦ These authors contributed equally to this work.
† The University of North Carolina at Chapel Hill.
‡ Stanford University.

(1) Li, G.; Shrotriya, V.; Huang, J. S.; Yao, Y.; Moriarty, T.; Emery, K.; Yang, Y. *Nat. Mater.* **2005**, *4*, 864–868.
(2) Ma, W. L.; Yang, C. Y.; Gong, X.; Lee, K.; Heeger, A. J. *Adv. Funct. Mater.* **2005**, *15*, 1617–1622.
(3) Peet, J.; Kim, J. Y.; Coates, N. E.; Ma, W. L.; Moses, D.; Heeger, A. J.; Bazan, G. C. *Nat. Mater.* **2007**, *6*, 497–500.
(4) van Duren, J. K. J.; Yang, X. N.; Loos, J.; Bulle-Lieuwma, C. W. T.; Sieval, A. B.; Hummelen, J. C.; Janssen, R. A. J. *Adv. Funct. Mater.* **2004**, *14*, 425–434.
(5) Yang, X.; Loos, J. *Macromolecules* **2007**, *40*, 1353–1362.
(6) Coakley, K. M.; Liu, Y. X.; Goh, C.; McGehee, M. D. *MRS Bull.* **2005**, *30*, 37–40.
(7) Greene, L. E.; Law, M.; Yuhas, B. D.; Yang, P. D. *J. Phys. Chem. C* **2007**, *111*, 18451–18456.
(8) Olson, D. C.; Piris, J.; Collins, R. T.; Shaheen, S. E.; Ginley, D. S. *Thin Solid Films* **2006**, *496*, 26–29.
(9) Olson, D. C.; Shaheen, S. E.; Collins, R. T.; Ginley, D. S. *J. Phys. Chem. C* **2007**, *111*, 16670–16678.
(10) Ravirajan, P.; Peiro, A. M.; Nazeeruddin, M. K.; Graetzel, M.; Bradley, D. D. C.; Durrant, J. R.; Nelson, J. *J. Phys. Chem. B* **2006**, *110*, 7635–7639.
(11) Coakley, K. M.; McGehee, M. D. *Chem. Mater.* **2004**, *16*, 4533–4542.

10.1021/cm800729q CCC: $40.75 
Published on Web 07/29/2008

accept electrons from almost all organic semiconductors,[12] and its surface can be easily functionalized with organic molecules that facilitate exciton dissociation and charge transfer.[13] Also, titania is well studied by the dye-sensitized solar cell community.[14,15]

The ideal titania nanostructure in an ordered heterojunction should be approximately 200−300 nm thick and consist of an ordered array of titania posts or pores with 10−20 nm spacing (approximately twice the polymer exciton diffusion length[16]), as illustrated in Figure 1b.[11] With this geometry, every exciton formed in the donor material is able to reach the interface and be split into two distinct charge carriers. The channels should also be straight and perpendicular to the substrate so that both charge carriers have a direct pathway to their respective electrode. Previously, titania nanostructures have been made using a variety of techniques, including doctor blade spreading of titania paste,[17] spray pyrolysis of titanium alkoxides,[18] and evaporation-induced self-assembly of titania solution precursors with an amphiphilic block copolymer as a structure-directing agent.[19–21] However, these methods do not produce straight channels that reach the back electrode. Instead, the pores are tortuous and the polymer chain packing is disrupted, decreasing hole mobility and thus reducing device performance.[19,22] Previous results using photovoltaic cells fabricated by infiltrating P3HT into mesoporous titania networks have shown that the polymer morphology within the porous network hinders charge transport to the electrodes.[23] Recently, in an attempt to fabricate straight $TiO_2$ pathways, anatase-phase $TiO_2$ nanorods were employed in a blend for use in conjunction with P3HT as a polymer−titania device.[24] One technique for optimizing the nanostructured morphology is nanoimprint lithography,[25–27] a promising method due to its high throughput capability to produce nanoscale features over a large area. Whitesides et al.[28–30] used polydimethylsiloxane (PDMS) molds to pattern sol−gel-derived inorganic oxides into continuous membranes with nanoscale features and into discrete objects at fractions of a millimeter length scale. After gelation of liquid sol−gel precursors, the PDMS molds were removed and the patterned structures were annealed at high temperature. While features as small as 30 nm have been reported, the process is limited by deformations such as feature coalescence, sagging, and swelling of the elastomeric PDMS mold. Another approach toward sub-100 nm pattern replication in titania employs polymethylmethacrylate (PMMA) molds with a PDMS backing layer for added flexibility.[31] The high compression modulus of PMMA prevents mold deformation and allows for higher resolution patterning. However, in this method, mold retrieval requires the wet etching of the master template followed by dissolving the mold away from the inorganic pattern. The nonreusable nature of the master and mold make this method unsuitable for manufacturing.

The use of perfluoropolyether (PFPE) elastomers as a reusable molding material for soft lithography has been reported by Rolland et al.[32,33] PFPE elastomers as a molding material are unique over their silicone-based counterparts in four distinctive ways: (i) the very low surface energy of PFPEs enables the selective filling of nanoscale cavities in the mold with almost any organic liquid; (ii) unlike silicones, fluoropolymers are resistant to swelling in common organic solvents, making them useful for patterning a wide range of organic and inorganic features; (iii) the chemical inertness of the PFPE molds allows the resultant array of features to be easily separated from the mold; and (iv) the modulus of the elastomer can be tuned by precursor molecular weight, allowing for patterning of a wide variety of sol−gels into sub-100 nm features. This process, referred to as PRINT (Pattern Replication In Nonwetting Templates) and shown in Figure 2, shows great potential for controlling device architecture in ordered bulk heterojunction solar cells. In this paper, we present the use of PRINT for patterning anatase $TiO_2$ on a sub-100 nm length scale. The ordered bulk heterojunction devices, made by infiltrating titania nanostructures with poly-3-hexylthiophene (P3HT), show a 2-fold improvement in short-circuit current relative to flat bilayer devices.

## Results and Discussion

**Fabrication of Master Template by Nanosphere Lithography and Production of PFPE Molds.** Nanosphere lithography (NSL) has proven to be a simple yet effective technique to obtain periodic arrays of nanopillars across a large surface area.[34] By first spin casting a dilute solution

(12) van Hal, P. A.; Christiaans, M. P. T.; Wienk, M. M.; Kroon, J. M.; Janssen, R. A. J. *J. Phys. Chem. B* **1999**, *103*, 4352–4359.
(13) Goh, C.; Scully, S. R.; McGehee, M. D. *J. Appl. Phys.* **2007**, *101*, 114503.
(14) Bach, U.; Lupo, D.; Comte, P.; Moser, J.; Weissortel, F.; Salbeck, J.; Spreitzer, H.; Gratzel, M. *Nature (London)* **1998**, *395*, 583–585.
(15) O'Regan, B.; Gratzel, M. *Nature* **1991**, *353*, 737–740.
(16) Scully, S. R.; McGehee, M. D. *J. Appl. Phys.* **2006**, *100*, 034907.
(17) Arango, A. C.; Carter, S. A.; Brock, P. J. *Appl. Phys. Lett.* **1999**, *74*, 1698–1700.
(18) Huisman, C. L.; Goossens, A.; Schoonman, J. *Chem. Mater.* **2003**, *15*, 4617–4624.
(19) Coakley, K. M.; Liu, Y. X.; McGehee, M. D.; Frindell, K. L.; Stucky, G. D. *Adv. Funct. Mater.* **2003**, *13*, 301–306.
(20) Alberius, P. C. A.; Frindell, K. L.; Hayward, R. C.; Kramer, E. J.; Stucky, G. D.; Chmelka, B. F. *Chem. Mater.* **2002**, *14*, 3284–3294.
(21) Crepaldi, E. L.; Soler-Illia, G. J. D. A.; Grosso, D.; Cagnol, F.; Ribot, F.; Sanchez, C. *J. Am. Chem. Soc.* **2003**, *125*, 9770–9786.
(22) Coakley, K. M.; Srinivasan, B. S.; Ziebarth, J. M.; Goh, C.; Liu, Y. X.; McGehee, M. D. *Adv. Funct. Mater.* **2005**, *15*, 1927–1932.
(23) Coakley, K. M.; McGehee, M. D. *Appl. Phys. Lett.* **2003**, *83*, 3380–3382.
(24) Boucle, J.; Chyla, S.; Shaffer, M. S. P.; Durrant, J. R.; Bradley, D. D. C.; Nelson, J. C. R. *Phys.* **2008**, *9*, 110–118.
(25) Kim, M. S.; Kim, J. S.; Cho, J. C.; Shtein, M.; Guo, L. J.; Kim, J. *Appl. Phys. Lett.* **2007**, *90*, 123113.
(26) Nanditha, D. M.; Dissanayake, M.; Adikaari, A. A. D. T.; Curry, R. J.; Hatton, R. A.; Silva, S. R. P. *Appl. Phys. Lett.* **2007**, *90*, 253502.
(27) Her, H.-J.; Kim, J.-M.; Kang, C. J.; Kim, Y.-S. *J. Phys. Chem. Solids* **2008**, *69*, 1301–1304.
(28) Marzolin, C.; Smith, S. P.; Prentiss, M.; Whitesides, G. M. *Adv. Mater.* **1998**, *10*, 571–574.
(29) Yang, H.; Deschatelets, P.; Brittain, S. T.; Whitesides, G. M. *Adv. Mater.* **2001**, *13*, 54–58.
(30) Yang, P. D.; Deng, T.; Zhao, D. Y.; Feng, P. Y.; Pine, D.; Chmelka, B. F.; Whitesides, G. M.; Stucky, G. D. *Science* **1998**, *282*, 2244–2246.
(31) Goh, C.; Coakley, K. M.; McGehee, M. D. *Nano Lett.* **2005**, *5*, 1545–1549.
(32) Rolland, J. P.; Hagberg, E. C.; Denison, G. M.; Carter, K. R.; De Simone, J. M. *Angew. Chem., Int. Ed.* **2004**, *43*, 5796–5799.
(33) Rolland, J. P.; Van Dam, R. M.; Schorzman, D. A.; Quake, S. R.; DeSimone, J. M. *J. Am. Chem. Soc.* **2004**, *126*, 2322–2323.
(34) Hulteen, J. C.; Vanduyne, R. P. *J. Vac. Sci. Technol., A* **1995**, *13*, 1553–1558.

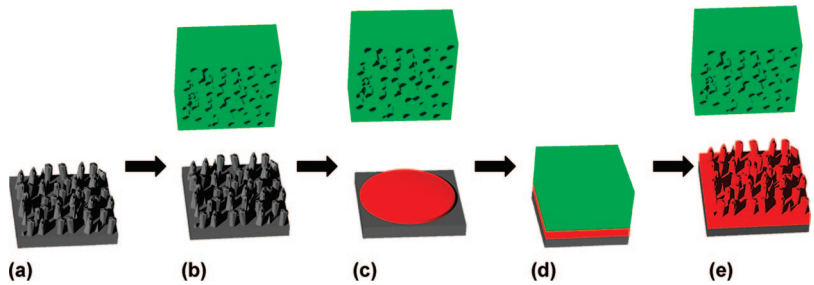


**Figure 2.** Illustration of the PRINT process: (a) Si master template; (b) mold release from master template; (c) molding a liquid precursor; (d) pattern transfer to substrate at elevated temperature and pressure; (e) mold release from replica film.

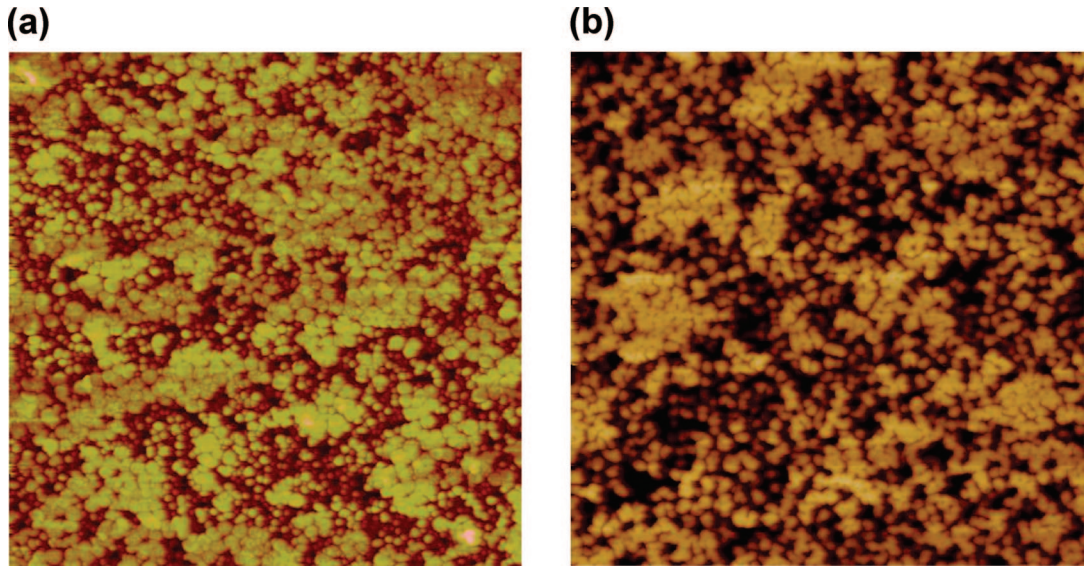


**Figure 3.** 3 × 3 $\mu$m atomic force microscope images of the (a) silicon master fabricated via nanosphere lithography and the (b) 1 kDa PFPE elastomer mold of the master template. $z$ height = 150 nm for both images.

of polystyrene nanospheres on a silicon wafer, a monolayer of nanospheres was readily deposited over the entire surface. These nanospheres are not robust enough to be used directly as an etch mask for reactive ion etching (RIE); therefore, a 5 nm Cr layer was deposited on top of the nanosphere monolayer using electron-beam evaporation. The nanospheres were then dissolved by sonication in toluene at 60 °C. This process leaves behind islands of Cr that are used as an etch mask for nanopillars. The height of the final features in silicon is directly proportional to the time of the RIE (all other conditions remaining constant). The features we obtained were randomly oriented postlike structures with the highest aspect ratio structures having a maximum height of 140 nm and a diameter of 20 nm. The random orientation was due to the large variance in nanosphere diameters (average of 20 nm), which resulted in various sized interstitial holes between nanospheres where the Cr mask was deposited. Any Cr remaining on top of the nanopillars was removed using a standard piranha etch. While the feature shape and distribution across the wafer varied for each sample, this method was effective in generating nanoscale patterns across a large area.

In order to obtain an elastomer mold of the NSL master template, a liquid PFPE precursor comprised of 1 kDa PFPE (α,Ω-functionalized dimethacrylate) and 2,2-diethoxyacetophenone was poured over the nanopatterned master template. Due to its very low surface energy, the liquid PFPE was capable of selectively filling the nanoscale cavities in the master. Subsequent photochemical cross-linking resulted in a high-fidelity mold of the nanoscale features of the NSL master template, as shown in Figure 3.

**Feature Replication in Anatase Titania.** When fabricating titania nanostructures for photovoltaic applications, it was necessary to employ two layers of titania on top of the fluorine-doped tin oxide (FTO) electrode. The first layer was a flat, thin film foundation of anatase titania upon which the nanostructured layer was fabricated. The first thin film of titania provided a pinhole-free layer that prevents device shorting as a result of direct pathways between the top and the bottom electrodes. This was especially important if the second (patterned) titania layer had any small cracks or pinholes. Different sol formulations were utilized for the two layers in order to obtain a crack-free thin film in the first layer and prevent volume reduction and feature degradation in the second layer.

In this process, a thin film of sol **1** as the compact underlayer was deposited onto fluorine-doped tin oxide (FTO) electrode by spin casting. The samples were then oven dried and calcined at 450 °C. Subsequently, liquid sol **2** was drop cast onto the sample and a PFPE mold was pressed down onto the substrate and held at constant pressure. The sample was heated to 110 °C to facilitate the sol−gel transition via solvent removal, a process that was aided by

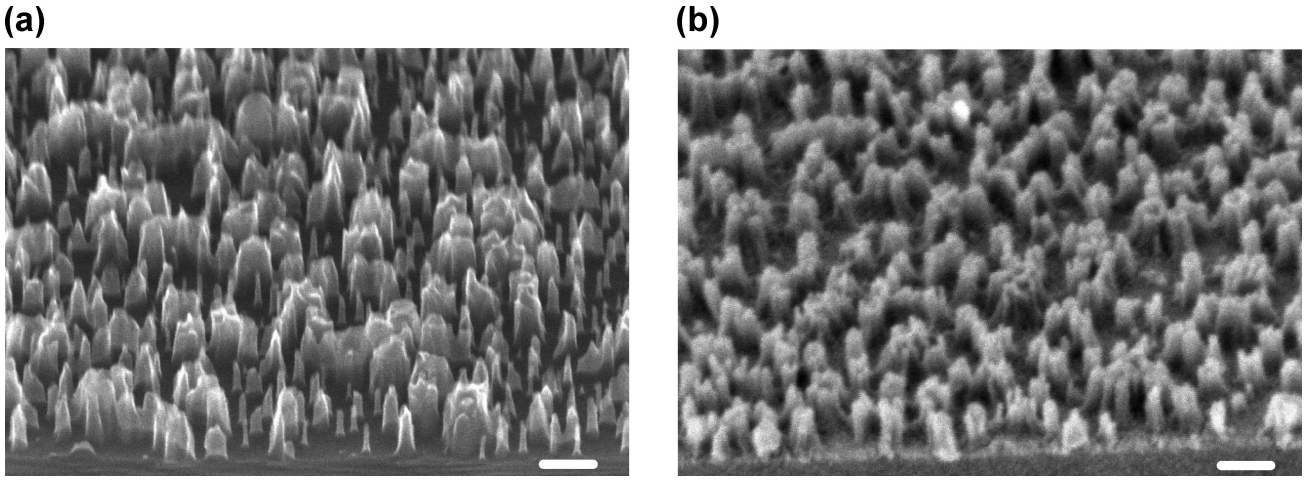


**Figure 4.** SEM image of (a) NSL silicon master template with 3-min RIE and (b) anatase titania nanostructure replicated using PRINT from the silicon master. Scale bars are 100 nm.

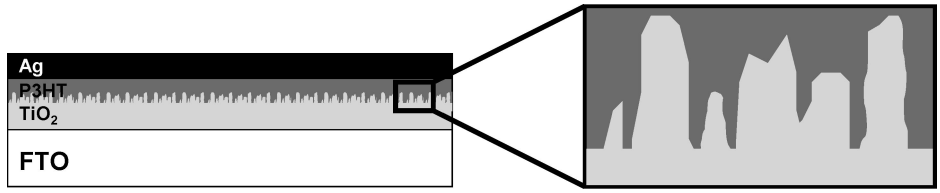


**Figure 5.** Schematic diagram showing the cross section of a photovoltaic device where the titania−polymer interface has been patterned using the PRINT technique.

the high permeability of the mold.[35] The low-surface energy PFPE mold was then peeled off the FTO substrate, leaving an embossed xerogel film. Calcination of the xerogel phase at 450 °C led to formation of anatase titania features (see Supporting Information). Scanning electron microscopy images of the silicon master template from NSL and resultant titania nanostructure are shown in Figure 4.

**Device Fabrication and Solar Cell Performance.** As previously described, we employed two layers of titania on top of the FTO electrode to fabricate the nanostructure. Reference cells were also fabricated with two layers of titania to ensure a comparable reference cell for the nanostructure devices. In this case, a thin film of titania was spun cast from sol **1** and calcined at 450 °C. A second film of titania was deposited by first drop casting sol **2** on the substrate and then placing a flat PFPE membrane on top of the sol. The substrate was held at elevated pressure and temperature for several hours, followed by PFPE membrane removal and 450 °C calcination of the sample.

After making nanostructured titania samples, a 100 nm thick P3HT layer was spun cast on top of the film and infiltrated around the features by heating the sample to 185 °C for 8 min in a nitrogen environment. According to previous studies by Coakley et al.[19,22] the annealing procedure should be sufficient to infiltrate P3HT to the bottom of the pores. Figure 5 is a schematic representation of the device stack for a nanostructure device.

Figure 6 shows the $I-V$ curves of the nanostructured titania devices along with the flat reference devices. We observed that incorporation of the interface modifier, Z907, helped improve the $J_{SC}$ and $V_{OC}$ for both reference and nanostructured devices. We attributed this enhancement to an improvement in exciton splitting at the interface. The carboxylic acid groups covalently bound to the titania surface promoted rapid forward electron transfer, while the long insulating alkyl side chains suppressed charge recombination and promoted wetting of the titania surface by the P3HT.[10,13,36–38]

When comparing devices that received the same interfacial treatments, nanostructuring of the titania increased the short-circuit current ($J_{SC}$) by 2-fold while maintaining the open circuit voltage ($V_{OC}$) relative to the flat film reference devices. As indicated in Table 1, upon nanostructuring, the $J_{SC}$ of the unmodified devices increased from 0.58 to 1.11 mA/cm$^2$, while for interface-modified devices the $J_{SC}$ increased from 0.83 to 1.73 mA/cm$^2$. This doubling of $J_{SC}$ agreed well with simple calculations based on increasing the titania/P3HT interfacial area for a hexagonal array of titania posts with dimensions of radius 10 nm, height 100 nm, and periodicity of 60 nm. Though the increase in photocurrent can be attributed solely to the increase in interfacial area, it is important to recognize that PRINT allows for straight, narrow pores to be fabricated which can lead to improved device performance. For example, charge mobility in the polymer phase can be enhanced due to chain alignment in the nanoscale channels of the nanostructure titania, which would result in an increased $J_{sc}$ and fill factor (F.F.).[22]

(35) Brinker, C. J. *The Physics and Chemistry of Sol-Gel Processing*, 1st ed.; Academic Press:San Diego, CA, 1990.
(36) Bartholomew, G. P.; Heeger, A. J. *Adv. Funct. Mater.* **2005**, *15*, 677–682.
(37) Schmidt-Mende, L.; Kroeze, J. E.; Durrant, J. R.; Nazeeruddin, M. K.; Gratzel, M. *Nano Lett.* **2005**, *5*, 1315–1320.
(38) Wang, P.; Zakeeruddin, S. M.; Moser, J. E.; Nazeeruddin, M. K.; Sekiguchi, T.; Gratzel, M. *Nat. Mater.* **2003**, *2*, 498–498.

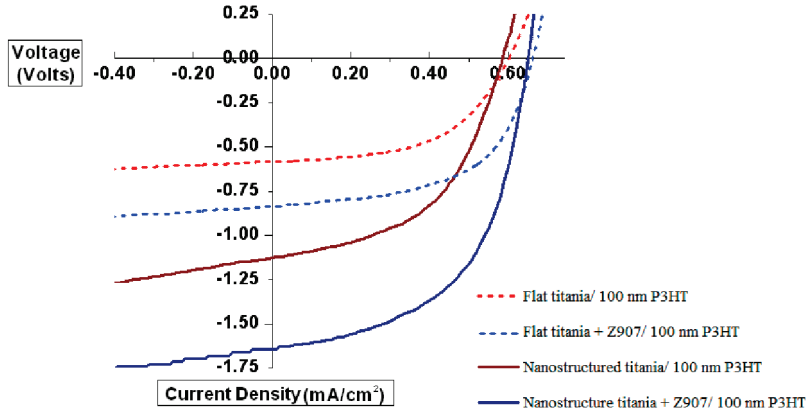


**Figure 6.** Current−voltage ($I-V$) curves of four titania/P3HT systems: flat titania/100 nm P3HT (reference device), flat titania with a surface modified with Z907/100 nm P3HT (reference device), nanostructured titania/100 nm P3HT, and nanostructured titania with surface modified with Z907/100 nm P3HT.

**Table 1. Photovoltaic Device Performance of Flat Titania/P3HT Devices and PRINT-Fabricated Nanostructured Devices for Z-907 Dye-Functionalized and Nonfunctionalized Devices**

| | $J_{sc}$ (mA/cm$^2$) | $V_{oc}$ (V) | F.F. | efficiency (%) |
|---|---|---|---|---|
| flat titiania/P3HT | 0.58 | 0.58 | 0.55 | 0.19 |
| nanostructured Titania/P3HT | 1.11 | 0.58 | 0.51 | 0.33 |
| flat titania + Z907/ P3HT | 0.83 | 0.64 | 0.58 | 0.31 |
| nanostructured titania + Z907/P3HT | 1.73 | 0.65 | 0.55 | 0.61 |

## Conclusions

We reported on the use of nanosphere lithography to make silicon master templates and the PRINT process to replicate the master template structures into anatase titania. We fabricated ordered bulk heterojunction solar cells with nanostructured titania and P3HT. Compared to a flat reference bilayer device, the short-circuit current was doubled upon nanostructuring while the open-circuit voltage remained the same. The nanostructured device with the Z907 interfacial modification led to a power conversion efficiency of 0.6%. This paper demonstrates the feasibility of fabricating nanostructured titania solar cells via PRINT, a potentially high-throughput soft lithography route that is amenable to a wide variety of materials and processing conditions. Additionally, further improvement in PV device efficiency could result from using a master template with higher aspect ratios and closer feature spacing and from infiltrating nanostructures with different materials such as low bandgap polymers. We fabricated a master template with smaller feature sizes, a higher degree of order, and controlled feature aspect ratios using block copolymer lithography. However, new challenges have been encountered when using these master templates for pattern replication in titania. Specifically, the height of the amorphous titania patterns does not match the original master template. Characterization of the PFPE molds indicates that they replicate the master template with a high degree of fidelity. We suspect that the titania sol−gel does not fill the PFPE mold or that it is damaged when the mold is pulled away. Reformulating the sol−gel may solve these problems. Once these challenges have been overcome, ordered BHJ photovoltaic devices with patterns closer to the ideal excitonic length scale will be fabricated and tested.

## Experimental Section

All chemicals were purchased from Aldrich except the Z907 dye, which was purchased from Solaronix SA. All chemicals were used as received except poly-3-hexylthiophene (P3HT), which was purified by Soxhlet extraction using hexane and then chloroform. The synthesis of perfluoropolyether dimethacrylate (PFPE DMA) has been reported previously.[32] The photoinitiator used to cure the PFPE DMA was 2,2-diethoxyacetophenone (DEAP). Metal oxides were characterized with an X-ray diffractometer (XRD, Rigaku) using Cu Kα radiation. XRD data can be found in the Supporting Information. SEM micrographs were obtained with either a Hitachi S-4700 instrument or a FEI Helios 600 NanoLab Dual Beam System.

**Nanosphere Lithography (NSL) Master Template Fabrication.** A monolayer of polystyrene nanospheres (diameter 26 ± 5.5 nm, concentration 4.1 g/100 mL, purchased from Interfacial Dynamics Corp.) was deposited on a silicon wafer by first diluting the original solution of nanospheres 2-fold and then spin casting at 5000 rpm. A 5 nm layer of Cr was evaporated on the nanosphere monolayer using electron-beam evaporation. The spheres were then dissolved by sonication in heated toluene for 1−2 h. The exposed silicon surface was etched using $NF_3$ reactive ion etching (RIE) (20 sccm $NF_3$, 20 mTorr chamber pressure, 430 V bias voltage) in an AMT 8100 Plasma Etcher. RIE times of 3 and 4 min were used. The nanopillar surface was cleaned using a UV−ozone treatment. Any remaining Cr was removed using a standard piranha etch (80% conc. sulfuric acid and 20% hydrogen peroxide, by volume). A similar process using a block copolymer as the etching mask was reported elsewhere.[39]

**PFPE Mold and Membrane Fabrication.** A liquid 1 kDa PFPE DMA (α,Ω-functionalized dimethacrylate) precursor solution containing 1 wt % 2,2-diethoxyacetophenone (DEAP) was poured over a NSL patterned master template or a piranha cleaned silicon wafer. The liquid precursor was then cross-linked using UV photoirradiation ($\lambda$ = 365 nm) for 3 min under a constant nitrogen purge to provide an elastomeric mold of the master template. The fully cured PFPE DMA elastomeric mold or flat membrane was then released from the respective silicon master or wafer.

**Sol−Gel Synthesis.** To make titania sol **1**, a 0.46 mL portion of titanium ethoxide was combined with 5.1 mL of 2-propanol. After several minutes of stirring, 0.18 mL of concentrated hydrochloric acid was added dropwise to the solution. The sol was stirred for 1 h and filtered through a 0.45 $\mu$m filter before use. To make titania

(39) Gowrishankar, V.; Miller, N.; McGehee, M. D.; Misner, M. J.; Ryu, D. Y.; Russell, T. P.; Drockenmuller, E.; Hawker, C. J. *Thin Solid Films* **2006**, *513*, 289–294.

sol **2**, 9.0 mL of titanium butoxide was combined with 0.27 mL of acetylacetone. After stirring for 15 min, 0.20 mL of 2-propanol was added to the solution. A 0.075 mL portion of glacial acetic acid was added dropwise to the stirrring solution. The sol was stirred for 1 h and filtered through a 0.45 $\mu$m filter before use.

**Titania Nanostructure Fabrication.** The glass/FTO substrates (AFG Industries Inc., 100 Ω/square) were cleaned by first scrubbing with a dilute solution of Contrex AP detergent, rinsed with DI $H_2O$, followed by sequential sonication in acetone and isopropanol. After drying the substrates at 110 °C in air and UV−ozone cleaning them for 15 min, a thin film of sol **1** was deposited by spin casting the sol at 2000 rpm. These samples were then oven dried at 110 °C for 12 h prior to being calcined at 450 °C for 30 min using a ramp rate of 5 °C/min. Sol **2** was then drop cast onto the substrate, and either a flat PFPE membrane or a patterned PFPE mold was pressed into the liquid sol. The sample was held at constant pressure at 110 °C for several hours. The mold was removed, and the samples were heated to 450 °C at a rate of 10 °C/min and held at 450 °C for 30 min to crystallize titania.

**Device Fabrication.** The freshly calcined titania was treated with a UV−ozone clean for 10 min. Subsequently, a layer of heat-curable polyimide was applied to one edge of the titania film. The polyimide was heated for 10 min each at 60, 90, and 140 °C, after which it was cured. The nondye-coated samples were promptly transferred into a glovebox filled with nitrogen. Some samples were first treated with the interfacial modifier (Z907), as reported previously,[13] before being transferred into the glovebox. For both the nanostructured and reference devices, a 100 nm thick P3HT film was spun cast from THF on top of the titania structures and melt infiltrated by heating at 185 °C in glovebox for 8 min followed by slow cooling.[19] Reflective top electrodes consisting of a 70 nm layer of Ag were then thermally evaporated under vacuum (at greater than $10^{-6}$ torr) on top of the polymer film. The use of shadow masks allowed us to fabricate six 3-mm$^2$ finger-like devices per substrate. All subsequent device testing experiments were done in a nitrogen environment.

**Acknowledgment.** This work was partially supported by the National Science Foundation under agreement no. CMS-0507151, NASA grant NAG-1-2301, Office of Naval Research, the STC program of the National Science Foundation under agreement no. CHE-9876674, the Army Research Office, the University of North Carolina Institute of Advanced Materials, the Global Climate and Energy Project at Stanford University, Liquidia Technologies, and the William R. Kenan, Jr., Distinguished Professorship. M.H. is supported by The Institute for the Environment of the University of North Carolina at Chapel Hill through a Carolina Energy Fellowship. I.K.D. is supported by a Stanford Graduate Fellowship. We acknowledge the help of P. White (X-ray diffractometer) and Kevin Herlihy for help with figures. We thank Dr. Zhilian Zhou, Liquidia Technologies, for useful discussions. S.S.W. and M.J.H. contributed equally to this work.

**Supporting Information Available:** XRD pattern for titania sol−gels and calculations for the increased interfacial area of nanostructured titania (PDF). This material is available free of charge via the Internet at http://pubs.acs.org.

CM800729Q